Published in final edited form as:
Cancer. 2010 January 15; 116(2): 451–458. doi:10.1002/cncr.24755.

Quantitative F18-Fluorodeoxyglucose Positron Emission Tomography Accurately Characterizes Peripheral Nerve Sheath Tumors as Malignant or Benign

Matthias R. Benz, MD[1,2], **Johannes Czernin, MD**[1,2], **Sarah M. Dry, MD**[3], **William D. Tap, MD**[4], **Martin S. Allen-Auerbach, MD**[1,2], **David Elashoff, PhD**[5], **Michael E. Phelps, PhD**[1,2], **Wolfgang A. Weber, MD**[6], and **Fritz C. Eilber, MD**[1,2,7]

[1]Department of Molecular Pharmacology, University of Freiburg, Freiburg, Germany

[2]Department of Medical Pharmacology, University of Freiburg, Freiburg, Germany

[3]Department of Pathology, University of Freiburg, Freiburg, Germany

[4]Division of Medical Oncology, University of Freiburg, Freiburg, Germany

[5]Department of Biostatistics, University of Freiburg, Freiburg, Germany

[6]Department of Nuclear Medicine, University of Freiburg, Freiburg, Germany

[7]Division of Surgical Oncology, University of California Los Angeles, Los Angeles, California

Abstract

BACKGROUND—Correct pretreatment classification is critical for optimizing diagnosis and treatment of patients with peripheral nerve sheath tumors (PNSTs). The aim of this study was to evaluate whether F18-fluorodeoxyglucose positron emission tomography (FDG PET) can differentiate malignant (MPNST) from benign PNSTs.

METHODS—Thirty-four adult patients presenting with PNST who underwent a presurgical FDG PET/computed tomography (CT) scan between February 2005 and November 2008 were included in the study. Tumors were characterized histologically, by FDG maximum standardized uptake value (SUV_{max} [g/mL]), and by CT size (tumor maximal diameter [cm]). The accuracy of FDG PET for differentiating MPNSTs from benign PNSTs (neurofibroma and schwannoma) was evaluated by receiver operating characteristic (ROC) curve analysis.

RESULTS—SUV_{max} was measured in 34 patients with 40 tumors (MPNSTs: n = 17; neurofibromas: n = 9; schwannomas: n = 14). SUV_{max} was significantly higher in MPNST compared with benign PNST (12.0 ± 7.1 vs 3.4 ± 1.8; $P < .001$). An SUV_{max} cutoff point of ≥6.1 separated MPNSTs from BPSNTs with a sensitivity of 94% and a specificity of 91% ($P < .001$). By ROC curve analysis, SUV_{max} reliably differentiated between benign and malignant PNSTs (area under the ROC curve of 0.97). Interestingly, the difference between MPNSTs and schwannomas was less prominent than that between MPNSTs and neurofibromas.

CONCLUSIONS—Quantitative FDG PET imaging distinguished between MPNSTs and neurofibromas with high accuracy. In contrast, MPNSTs and schwannomas were less reliably distinguished. Given the difficulties in clinically evaluating PNST and in distinguishing benign

Corresponding author: Fritz C. Eilber, MD, UCLA, Division of Surgical Oncology, 10833 Le Conte Avenue, Rm 54-140 CHS, Los Angeles, CA 90095-1782; Fax: (310) 825-7575; fceilber@mednet.ucla.edu.

CONFLICT OF INTEREST DISCLOSURES

PNST from MPNST, FDG PET imaging should be used for diagnostic intervention planning and for optimizing treatment strategies.

Keywords

positron emission tomography; computed tomography; malignant peripheral nerve sheath tumor; schwannoma; neurofibroma

Peripheral nerve sheath tumors (PNSTs) are benign or malignant neoplasms that arise from peripheral nerves. They include, among others, schwannoma and neurofibroma and their malignant variants. Several hereditary syndromes are associated with PNST. Neurofibromatosis type 1 (von Recklinghausen disease) is the most important known risk factor for the development of malignant PNST (MPNST), as about 50% of these occur in patients with neurofibromatosis type 1.[1] Notably, neurofibromatosis type 1 patients carry an up to 10% lifetime risk of developing MPNST, compared with a risk of <0.1% in the general population.[2,3]

MPNST is the sixth most common type of soft tissue sarcoma (STS), accounts for 3% to 10% of all STS,[2,4,5] is highly malignant, and carries a poor prognosis.[1,6,7] Another hereditary disease, neurofibromatosis type 2, is associated with schwannoma.[8]

Differentiating MPNST from benign PNST such as neurofibroma and schwannoma is difficult, particularly in patients with neurofibromatosis type 1. First, neurofibromatosis type 1 patients frequently have synchronous benign and malignant PNSTs. Second, multiple PNSTs (ranging in number from 2 to >10) are characteristic of neurofibromatosis type 1. Third, PNSTs in neurofibromatosis type 1 can arise in sites that are not amenable to biopsy. Fourth, even if a biopsy is feasible, sampling errors can occur, because these tumors are quite heterogeneous with benign and malignant areas present within 1 lesion. Fifth, malignant degeneration is not necessarily associated with changes in clinical symptoms. Finally, existing cross-sectional imaging modalities, including computed tomography (CT) and magnetic resonance imaging (MRI), can define the anatomic extent of the lesions, but cannot reliably distinguish malignant from benign PNST.[9,10]

The concept of using glucose metabolic positron emission tomography (PET) imaging with F18-fluorodeoxyglucose (FDG) as a noninvasive metabolic biopsy was introduced several years ago. FDG PET imaging has been shown to be highly accurate (>90%) in correctly distinguishing malignant from benign chest and extrathoracic lesions that were equivocal for malignancy by biopsy.[11,12] A noninvasive metabolic biopsy that would reliably differentiate MPNST from benign PNST would provide an invaluable and critical mechanism for managing patients with PNST.

The aim of this study was to evaluate the ability of FDG PET/CT to distinguish benign from malignant PNST in a large group of patients. Furthermore, we assessed whether sporadic and hereditary MPNST, schwannoma, and neurofibroma exhibit different glucose metabolic phenotypes.

MATERIALS AND METHODS

From February 2005 to November 2008, 34 adult patients (≥18 years old) with PNST were enrolled in the study. The study population consisted of 34 patients with 40 tumors for which pathology was available. There were 20 men and 14 women with a mean age of 46 years (range, 21–82 years). Twenty-five (74%) subjects were enrolled in prospective study protocols that were approved by the University of California Los Angeles Institutional Review Board. Nine (26%) patients had undergone a clinical FDG PET/CT study and were

enrolled retrospectively after the institutional review board had granted a waiver of the consent requirement.

PET/CT Image Acquisition and Reconstruction

PET/CT imaging was performed on the Siemens (Erlangen, Germany) Biograph Duo PET/CT scanner that consists of an ECAT ACCEL and dual detector helical CT scanner. Patients were instructed to fast for at least 6 hours before FDG PET imaging to standardize blood glucose and insulin levels. Blood glucose levels measured before injection of FDG ranged from 70 mg/dL to 105 mg/dL.

For CT imaging, intravenous (IV) contrast (Omnipaque; GE Healthcare, Waukesha, Wis) was administered in 29 of 34 patients at a rate of 2 mL per second 30 to 40 seconds before imaging commenced. In the remaining patients, CT images were acquired without IV contrast because of elevated creatinine levels or the recent administration of IV contrast.

The CT acquisition parameters were 130 kVp, 120 mA, 1-second tube rotation, 4-mm slice collimation, and a bed speed of 8 mm/second. To minimize misregistration between the CT and PET images, patients were instructed to use shallow breathing throughout the image acquisition.[13]

Approximately 60 minutes before image acquisition, patients were injected with 0.21 mCi/kg of FDG. The PET emission scan duration ranged from 1 to 5 minutes/bed position depending on the patient's body weight.[14,15] The CT images were reconstructed using conventional filtered back-projection, at 3.4-mm axial intervals to match the slice separation of the PET data. PET images were reconstructed using iterative algorithms (ordered-subset expectation maximum, 2 iterations, 8 subsets). The CT data were also used to correct for photon attenuation.[16]

PET/CT Image Analysis

FDG PET/CT images were analyzed by 1 observer. The Mirada workstation (REVEALMVS; CTI Mirada Solutions, Oxford, UK) was used to view PET and CT images and to measure tumor FDG uptake and the maximum tumor diameter. The maximum standardized uptake value (SUV_{max} [g/mL]) was evaluated in all histopathologically proven lesions as previously described.[17] SUV_{max} was used as a measure of tumor glucose utilization, as this parameter allows the best comparison between studies because of high reproducibility and low interobserver variability.[17]

Pathology Assessments

Specimens were reviewed by a pathologist with specialty training in sarcoma pathology (S.M.D.). Standard diagnostic criteria were used.[5] Briefly, neurofibroma was diagnosed for lesions showing spindled cells with tapered nuclei set in a matrix containing collagen fibers of various thicknesses; in addition, immunohistochemical stains showed scattered S100 protein positivity.[18] Schwannomas were also composed of spindled cells with tapered nuclei. However, they were characterized by hyper- and hypocellular regions, areas of palisaded nuclei (Verocay bodies) and hyalinized blood vessels, and an S100 stain that was strongly and diffusely positive. In both neurofibroma and schwannoma, mitoses were absent or sparse (no more than 1 of 10 high-power fields [HPFs]). In contrast, MPNSTs showed high cellularity, nuclear anaplasia, obvious mitoses (usually >20–10 HPFs), and necrosis. In patients without neurofibromatosis type 1, a diagnosis of MPNST was made only if the tumor arose from a nerve trunk or from a pre-existing benign PNST.

All 40 lesions had a pathologically confirmed diagnosis.

Statistical Analysis

Quantitative data are presented as mean ± standard deviation and range. The Mann-Whitney test was used for unpaired comparisons between quantitative parameters. The significance of the association between 2 variables was examined by using Fisher exact test. We used receiver operating characteristic (ROC) curves to define the optimum cutoff values for SUV_{max}. The optimum cutoff value for differentiation of malignancy was defined as the point on the ROC curve with the minimum distance from the 100% true-positive and the 0% false-positive rate. *P* values <.05 were considered statistically significant. Statistical analyses were performed using SPSS software for Windows (version 14.0, SPSS Inc., Chicago, Ill), Statistica V8.0 for Windows (StatSoft, Inc., Tulsa, Okla), and Graphpad Prism software for Windows (version 5.00, GraphPad Software Inc., La Jolla, Calif).

RESULTS

Pathology Findings

There were 17 (42.5%)MPNSTs and 23 benign (57.5%) PNSTs. Two patients had both malignant and benign PNST. Sixteen (94%) of the MPNSTs were high grade, and 1 (6%) was intermediate grade (French Federation of Cancer Centers Sarcoma Group grading system). Among the benign PNSTs, 9 (39%) were neurofibromas and 14 (61%) were schwannomas (Table 1).

The most common site of disease was the retroperitoneum/abdomen (n = 16, 40%) followed by chest/trunk (n = 13, 32.5%) and extremity (n = 11, 27.5%). Twelve (71%) MPNSTs were classified as sporadic disease, and 5 (29%) MPNSTs developed in patients with neurofibromatosis type 1.

Tumor Size by CT

As a group, MPNSTs were significantly larger than the benign variants (mean: 7.4 ± 4.1 cm vs 4.8 ± 2.7 cm; *P* = .008) (Table 1). However, the range in size of the benign and malignant tumors showed considerable overlap (Table 1; Fig. 1). An ROC analysis revealed that CT tumor size measurements could not reliably distinguish between malignant and benign PNSTs (area under the curve = 0.74) (Fig. 2). Tumor size did not differ significantly between sporadic and neurofibromatosis type 1-associated MPNSTs (*P* = .38) or between neurofibroma and schwannoma (*P* = .69). Maximum tumor diameters are listed in Table 1.

Tumor Glucose Metabolic Activity

The mean SUV_{max} for MPNSTs was significantly higher than that for benign PNSTs (mean: 12.0 ± 7.1 vs 3.4 ± 1.8 g/mL; *P* < .001) (Table 1; Fig. 1). Sporadic and neurofibromatosis type 1-associated MPNSTs showed comparable FDG uptake (mean: 11.7 ± 6.8 vs 12.8 ± 8.6 g/mL; *P* = 1.0). Among benign tumors, schwannomas exhibited a significantly higher SUV_{max} than neurofibromas (mean: 4.2 ± 1.9 vs 2.3 ± 0.7 g/mL; *P* = .004) (Table 1).

ROC analysis showed that the optimum threshold for separating malignant from benign tumors was an SUV_{max} of 6.1 g/mL. This resulted in an area under the ROC curve of 0.97 (Fig. 2) and a sensitivity and specificity for malignancy of 94% and 91%, respectively.

Two schwannomas exhibited SUVs >6.1 g/mL (SUV_{max} = 7.6 and 8.3 g/mL, respectively), and 1 patient with a sporadic MPNST had an SUV_{max} of <6.1 g/mL. Therefore, the positive and negative predictive values for malignancy by FDG PET were 89% and 95%, and the diagnostic accuracy was 93% (*P* < .001).

DISCUSSION

To our knowledge, this is the largest study to demonstrate the ability of FDG PET imaging to differentiate neurofibromas and schwannomas from malignant PNSTs. The current findings have several important clinical implications. First, noninvasive tools for detecting malignancy are critical, because patients with neurofibromatosis type 1 carry a 10% lifetime risk of developing MPNST,[3] typically have multiple simultaneous PNSTs, and usually develop synchronous MPNSTs and benign PNSTs. This malignant degeneration cannot be reliably detected using clinical symptoms, anatomical imaging, or, because of sampling errors, even biopsy. Because of these limitations, malignant degeneration is often identified late in the course of the disease, compromising the potential for cure.

Currently, anatomical imaging (CT or MRI) is the standard technique for diagnosing and surveying PNSTs. In this study, ROC analysis revealed that CT was significantly less accurate than FDG PET for characterizing tumors as malignant or benign (Fig. 2).

Our results in this large patient population support prior observations that PET can differentiate benign PNSTs from MPNSTs in neurofibromatosis type 1 patients.[19–23] In the largest study,[20] FDG PET diagnosed neurofibromatosis type 1-associated MPNST with a sensitivity of 89% and a specificity of 95%. This is consistent with our observations in both sporadic and neurofibromatosis type 1-associated PNSTs.

FDG PET accurately identified a MPNST arising from a benign PNST in 1 of the neurofibromatosis type 1 patients (Fig. 3). This patient had several PNSTs, including 1 in the right distal thigh that, similar to this patient's other PNSTs, had shown slight growth over time. Given the large size of this lesion, biopsy was recommended and showed only a benign neurofibroma. However, PET showed a heterogeneous tumor with a large area of markedly increased FDG uptake (SUV_{max} = 14.9 g/mL), with much lower uptake elsewhere in the tumor and in a PNST in the contralateral thigh. The resected right distal thigh mass demonstrated a high-grade MPNST arising from a benign neurofibroma (Fig. 3). Thus, in this patient, FDG PET accurately identified both components—the benign neurofibroma and the MPNST—within this single tumor. This case illustrates the potential contribution of PET imaging for optimal clinical management of patients with PNSTs.

Pretreatment classification of PNSTs dictates subsequent clinical interventions. Benign PNST patients can be followed with serial imaging or undergo nerve-sparing/function-sparing surgery. In contrast, patients with MPNST, an aggressive soft tissue sarcoma with a 5-year disease-specific mortality of up to 75%,[6] require radical surgical resection, radiation therapy, and often chemotherapy.[24,25] Our results indicate that PET imaging can differentiate benign PNSTs from MPNSTs with high sensitivity and specificity. Furthermore, PET imaging can assist in guiding targeted needle core biopsies of PNSTs, as in the above case. Finally, because of the high sensitivity and specificity, PET imaging may provide critical information in tumors that are not amenable to biopsy.

FDG uptake varied considerably among patients with MPNSTs. The current study did not attempt to elucidate the reasons for this variability. However, the substantial variability might in part be explained by differences in hypoxia-inducible factor-1α expression, as shown previously in soft tissue sarcomas.[26]

Currently, the diagnosis of MPNST is made pathologically. Unfortunately, even in experienced hands, targeted needle core biopsies are often technically not feasible or falsely negative because of the often heterogeneous nature of these tumors, which frequently exhibit large areas of necrosis. Furthermore, in many patients with neurofibromatosis type 1, benign and malignant lesions coexist, and therefore the appropriate target tissue for biopsy

frequently is unknown. In addition, clinical symptoms such as rapid increase in tumor size, neurological deficits, and pain, although suspicious, are not specific formalignancy.

Interestingly, the difference between malignant PNSTs and benign schwannomas was less prominent (Figs. 1 and 4). This was largely because of the finding that 3 of the 14 patients with schwannoma exhibited SUVs >5 g/mL. A substantial variability in FDG uptake by schwannoma has been reported previously.[27–29] In contrast to a previous report,[30] studies by our group did not find significant differences in proliferative rate (measured by maximal mitoses per 10 HPFs, Ki-67 rate, skp2 rate), apoptotic rate (measured by TUNEL staining), expression of markers of glucose utilization (glucose-transport protein 1 and hexokinase II), or degree of intratumoral lymphocytes between the PET-positive and PET-negative benign PNST cases in this study (data not shown) that could explain the differences in FDG uptake as shown in Figure 4. However, different factors such as the expression level of hypoxia-inducible factor-1α, not measured in these samples, might have contributed to different glucose metabolic phenotypes by FDG PET imaging.[31] Thus, although the mechanism for increased PET activity in schwannomas remains unclear, it is evident from this and prior studies that schwannomas are less reliably discriminated from MPNST by FDG PET imaging.

The role of metabolic imaging is rapidly evolving. We currently use FDG PET/CT in patients with suspected malignant PNST, particularly before surgery or biopsy. For surveillance, we perform FDG PET/CT scans every 6 months for the first 2 years and annually thereafter, if the clinical status is unchanged. Rarely do we use MRI. In addition, we have found that FDG PET can accurately monitor response to therapy in MPNST.[32,33]

Limitations of this study include that all but 1 of the patients with MPNST (intermediate grade; SUV_{max}: 8.3 g/mL) had high-grade tumors. Thus, it remains unclear whether FDG PET can reliably discriminate intermediate- and/or low-grade MPNST from benign tumors.

In summary, our study demonstrated that FDG PET can reliably discriminate MPNST from benign PNST and confirmed that size criteria, by CT imaging, cannot make this distinction. ROC curve analysis revealed that an SUV_{max} threshold of 6.1 g/mL differentiated malignant from benign PNST with a sensitivity and specificity of 94% and 91%, respectively. Lowering this threshold to 4.5 g/mL would have increased the sensitivity to 100% but reduced the specificity to 83%. Conversely, raising the threshold to 8.5 g/mL increased the specificity to 100% but reduced the sensitivity to 65%. These thresholds need to be applied prospectively in future PNST studies to determine the best thresholds and the true diagnostic accuracy of FDG PET. FDG PET imaging can play a critical role and should be considered in the treatment planning of patients with PNSTs.

Acknowledgments

This work was supported by UCLA ICMIC (5 P50 CA086306) and UCLA DOE (DE-FG02-06ER64249) grants.

REFERENCES

1. Grobmyer SR, Reith JD, Shahlaee A, Bush CH, Hochwald SN. Malignant peripheral nerve sheath tumor: molecular pathogenesis and current management considerations. J Surg Oncol. 2008; 97:340–349. [PubMed: 18286466]
2. Ducatman BS, Scheithauer BW, Piepgras DG, Reiman HM, Ilstrup DM. Malignant peripheral nerve sheath tumors. A clinicopathologic study of 120 cases. Cancer. 1986; 57:2006–2021. [PubMed: 3082508]
3. McGaughran JM, Harris DI, Donnai D, et al. A clinical study of type 1 neurofibromatosis in north west England. J Med Genet. 1999; 36:197–203. [PubMed: 10204844]

4. Vauthey JN, Woodruff JM, Brennan MF. Extremity malignant peripheral nerve sheath tumors (neurogenic sarcomas): a 10-year experience. Ann Surg Oncol. 1995; 2:126–131. [PubMed: 7728565]
5. Weiss, S.; Goldblum, J. Enzinger and Weiss's Soft Tissue Tumors. St. Louis, MO: Mosby; 2001.
6. Eilber FC, Brennan MF, Eilber FR, Dry SM, Singer S, Kattan MW. Validation of the postoperative nomogram for 12-year sarcoma-specific mortality. Cancer. 2004; 101:2270–2275. [PubMed: 15484214]
7. Eilber FC, Tap WD, Nelson SD, Eckardt JJ, Eilber FR. Advances in chemotherapy for patients with extremity soft tissue sarcoma. Orthop Clin North Am. 2006; 37:15–22. [PubMed: 16311108]
8. Wiestler, O.; Radner, H. Pathology of neurofibromatosis 1 and 2. In: Huson, SM.; Hughes, RAC., editors. The Neurofibromatosis: A Pathologic and Clinical Overview. Cambridge, UK: Chapman and Hall; 1994. p. 135-160.
9. Ferner RE, Gutmann DH. International consensus statement on malignant peripheral nerve sheath tumors in neurofibromatosis. Cancer Res. 2002; 62:1573–1577. [PubMed: 11894862]
10. Rha SE, Byun JY, Jung SE, Chun HJ, Lee HG, Lee JM. Neurogenic tumors in the abdomen: tumor types and imaging characteristics. Radiographics. 2003; 23:29–43. [PubMed: 12533638]
11. Beggs AD, Hain SF, Curran KM, O'Doherty MJ. FDG-PET as a "metabolic biopsy" tool in non-lung lesions with indeterminate biopsy. Eur J Nucl Med Mol Imaging. 2002; 29:542–546. [PubMed: 11914894]
12. Hain SF, Curran KM, Beggs AD, Fogelman I, O'Doherty MJ, Maisey MN. FDG-PET as a "metabolic biopsy" tool in thoracic lesions with indeterminate biopsy. Eur J Nucl Med. 2001; 28:1336–1340. [PubMed: 11585292]
13. Beyer T, Antoch G, Muller S, et al. Acquisition protocol considerations for combined PET/CT imaging. J Nucl Med. 2004; 45 suppl 1:25S–35S. [PubMed: 14736833]
14. Halpern BS, Dahlbom M, Auerbach MA, et al. Optimizing imaging protocols for overweight and obese patients: a lutetium orthosilicate PET/CT study. J Nucl Med. 2005; 46:603–607. [PubMed: 15809482]
15. Halpern BS, Dahlbom M, Quon A, et al. Impact of patient weight and emission scan duration on PET/CT image quality and lesion detectability. J Nucl Med. 2004; 45:797–801. [PubMed: 15136629]
16. Kinahan PE, Townsend DW, Beyer T, Sashin D. Attenuation correction for a combined 3D PET/CT scanner. Med Phys. 1998; 25:2046–2053. [PubMed: 9800714]
17. Benz MR, Evilevitch V, Allen-Auerbach MS, et al. Treatment monitoring by 18F-FDG PET/CT in patients with sarcomas: interobserver variability of quantitative parameters in treatment-induced changes in histopathologically responding and nonresponding tumors. J Nucl Med. 2008; 49:1038–1046. [PubMed: 18552153]
18. Weiss SW, Langloss JM, Enzinger FM. Value of S-100 protein in the diagnosis of soft tissue tumors with particular reference to benign and malignant Schwann cell tumors. Lab Invest. 1983; 49:299–308. [PubMed: 6310227]
19. Bredella MA, Torriani M, Hornicek F, et al. Value of PET in the assessment of patients with neurofibromatosis type 1. AJR Am J Roentgenol. 2007; 189:928–935. [PubMed: 17885067]
20. Ferner RE, Golding JF, Smith M, et al. [18F]2-Fluoro-2-deoxy-D-glucose positron emission tomography (FDG PET) as a diagnostic tool for neurofibromatosis 1 (NF1) associated malignant peripheral nerve sheath tumours (MPNSTs): a long-term clinical study. Ann Oncol. 2008; 19:390–394. [PubMed: 17932395]
21. Ferner RE, Lucas JD, O'Doherty MJ, et al. Evaluation of fluorodeoxyglucose positron emission tomography (FDG PET) in the detection of malignant peripheral nerve sheath tumours arising from within plexiform neurofibromas in neurofibromatosis 1. J Neurol Neurosurg Psychiatry. 2000; 68:353–357. [PubMed: 10675220]
22. Cardona S, Schwarzbach M, Hinz U, et al. Evaluation of F18-deoxyglucose positron emission tomography (FDG-PET) to assess the nature of neurogenic tumours. Eur J Surg Oncol. 2003; 29:536–541. [PubMed: 12875862]

23. Warbey VS, Ferner RE, Dunn JT, Calonje E, O'Doherty MJ. [18F]FDG PET/CT in the diagnosis of malignant peripheral nerve sheath tumours in neurofibromatosis type-1. Eur J Nucl Med Mol Imaging. 2009; 36:751–757. [PubMed: 19142634]
24. Eilber FC, Rosen G, Eckardt J, et al. Treatment-induced pathologic necrosis: a predictor of local recurrence and survival in patients receiving neoadjuvant therapy for high-grade extremity soft tissue sarcomas. J Clin Oncol. 2001; 19:3203–3209. [PubMed: 11432887]
25. Grobmyer SR, Maki RG, Demetri GD, et al. Neo-adjuvant chemotherapy for primary high-grade extremity soft tissue sarcoma. Ann Oncol. 2004; 15:1667–1672. [PubMed: 15520069]
26. Shintani K, Matsumine A, Kusuzaki K, et al. Expression of hypoxia-inducible factor (HIF)-1alpha as a biomarker of outcome in soft-tissue sarcomas. Virchows Arch. 2006; 449:673–681. [PubMed: 17103226]
27. Ahmed AR, Watanabe H, Aoki J, Shinozaki T, Takagishi K. Schwannoma of the extremities: the role of PET in preoperative planning. Eur J Nucl Med. 2001; 28:1541–1551. [PubMed: 11685498]
28. Beaulieu S, Rubin B, Djang D, Conrad E, Turcotte E, Eary JF. Positron emission tomography of schwannomas: emphasizing its potential in preoperative planning. AJR Am J Roentgenol. 2004; 182:971–974. [PubMed: 15039173]
29. Watanabe H, Inoue T, Shinozaki T, et al. PET imaging of musculoskeletal tumours with fluorine-18 alpha-methyltyrosine: comparison with fluorine-18 fluorodeoxyglucose PET. Eur J Nucl Med. 2000; 27:1509–1517. [PubMed: 11083540]
30. Salla JT, Johann AC, Lana AM, do Carmo MA, Nunes FD, Mesquita RA. Immunohistochemical study of GLUT-1 in oral peripheral nerve sheath tumors. Oral Dis. 2008; 14:510–513. [PubMed: 18826382]
31. Thomas GV, Tran C, Mellinghoff IK, et al. Hypoxia-inducible factor determines sensitivity to inhibitors of mTOR in kidney cancer. Nat Med. 2006; 12:122–127. [PubMed: 16341243]
32. Benz MR, Czernin J, Allen-Auerbach MS, et al. FDG-PET/CT imaging predicts histopathologic treatment responses after the initial cycle of neoadjuvant chemotherapy in high-grade soft-tissue sarcomas. Clin Cancer Res. 2009; 15:2856–2863. [PubMed: 19351756]
33. Evilevitch V, Weber WA, Tap WD, et al. Reduction of glucose metabolic activity is more accurate than change in size at predicting histopathologic response to neoadjuvant therapy in high-grade soft-tissue sarcomas. Clin Cancer Res. 2008; 14:715–720. [PubMed: 18245531]

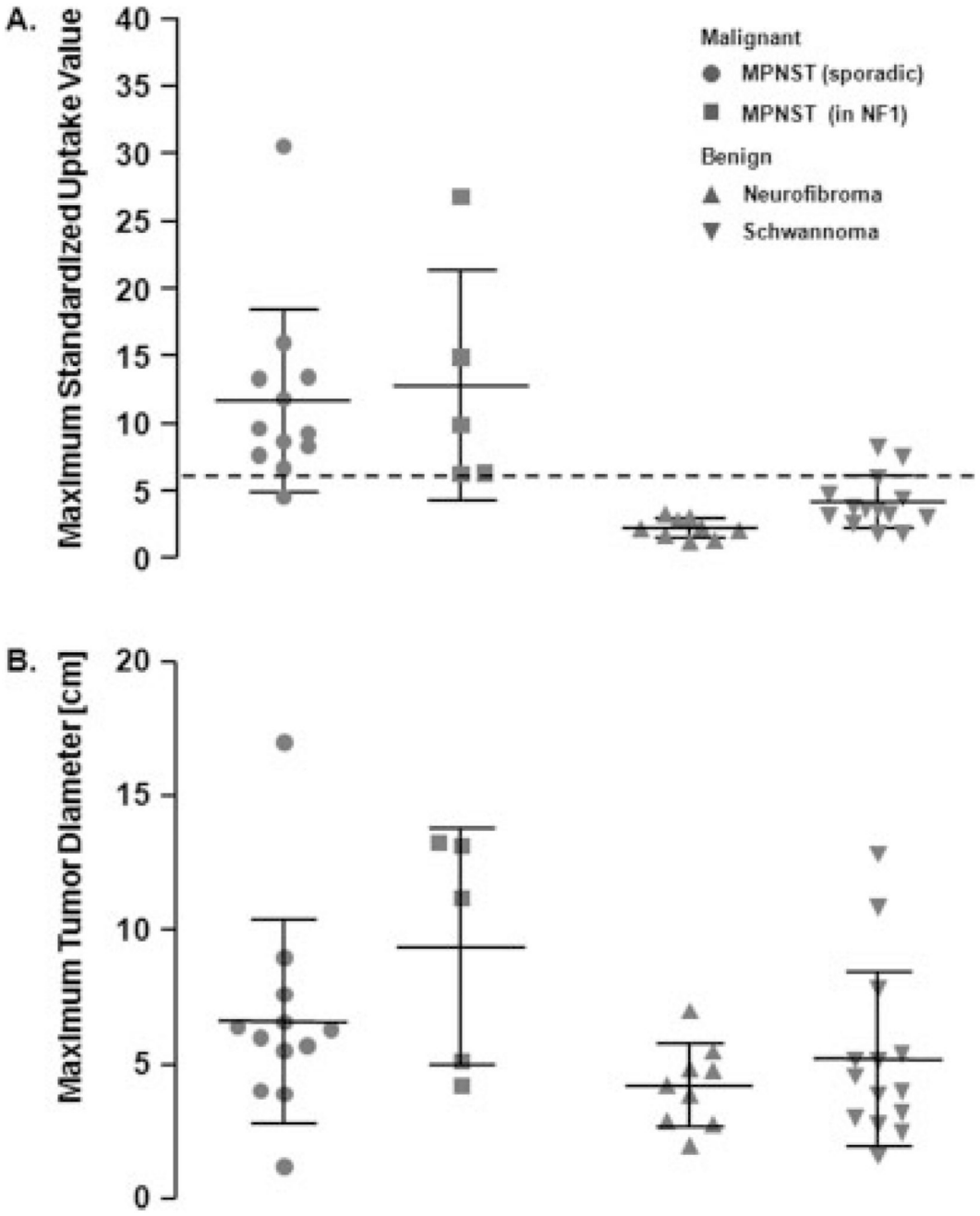

Figure 1.

(A) The maximum standard uptake value (SUV_{max}) of each lesion is represented by 1 symbol. Mean and standard deviation are depicted for each group. The mean SUV_{max} of malignant peripheral nerve sheath tumors (MPNSTs) was significantly higher than that of benign PNSTs ($P < .001$). A cutoff value of 6.1 identified 16 of 17 malignant PNSTs as true positive and 21 of 23 benign lesions as true negative (sensitivity, 94%; specificity, 91%; accuracy, 93%). (B) The corresponding maximum tumor diameters of each lesion are depicted. MPNSTs were significantly larger than the benign variants ($P = .008$). However, there was considerable overlap in tumor size between malignant and benign tumors. NF1 indicates neurofibromatosis type 1.

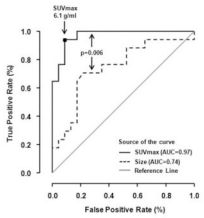

Figure 2.

Receiver operating characteristic (ROC) curves for assessment of malignancy by tumor metabolic activity (solid line) and tumor size (dotted line) are shown. The gray line indicates the expected ROC curve for random guessing of malignancy. SUV_{max} indicates maximum standard uptake value; AUC, area under the curve.

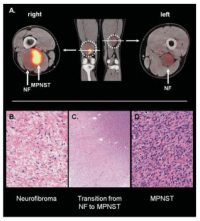

Figure 3.

(A) A positron emission tomography/computed tomography study in a patient with neurofibromatosis (NF) type 1-associated malignant peripheral nerve sheath tumor (MPNST) is depicted. The MPNST is located in the right distal thigh (maximum standard uptake value [SUV_{max}], 14.9) and arises from a benign neurofibroma. A neurofibroma with lower F18-fluorodeoxyglucose uptake (SUV_{max}, 2.3) is located in the left medial thigh. (B–D) The histologic findings of the patient's right thigh lesion are depicted. (B) A region of benign neurofibroma (original magnification, ×20) shows the usual low cellularity and slender spindled cells with interspersed pink collagen fibers. Note that no mitoses or necrosis is present. (C) A low-power view (original magnification, ×2) shows transition from neurofibroma (lower left corner) to high-grade MPNST (upper right corner). Note the increase in cellularity from the benign to the malignant area. (D) A high-power view (original magnification, ×20) of the high-grade MPNST is shown. Note the marked increase in cellularity, obvious mitoses, and nuclear pleomorphism. Extensive necrosis (not pictured here) was also present.

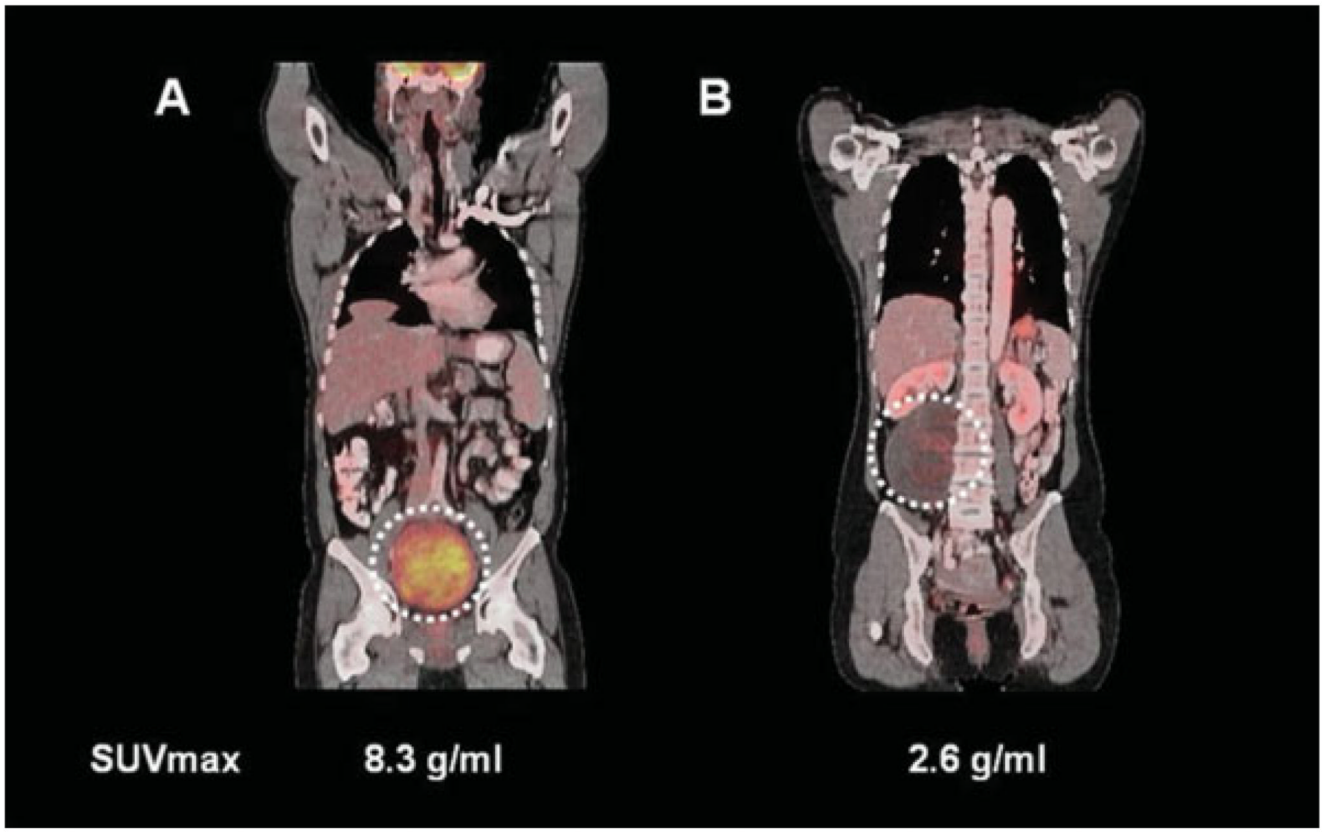

Figure 4.
(A) A schwannoma with high F18-fluorodeoxyglucose (FDG) uptake located in the pelvis is depicted. (B) By comparison, a patient with a schwannoma located in the right retroperitoneum with low FDG uptake is shown. This illustrates the wide range of maximum standardized uptake value (SUV_{max}) among schwannomas. Despite an extensive histopathologic and immunohistochemical analysis, we could not detect differences that could account for the divergent FDG uptake of these 2 schwannomas.

Table 1

Imaging Findings

	Malignant				Benign						
Tumor Type	**Total**	**Sporadic**	**NF1**	***P* Sporadic vs NF1**	**Total**	**NF**	**SWN**	***P* NF vs SWN**	***P* Malignant vs Benign**	***P* Malignant vs NF**	***P* Malignant vs SWN**
Number	17	12	5	—	23	9	14	—	—	—	—
SUV_{max}, g/mL[a]	12.0±7.1	11.7±6.8	12.8±8.6	1.0	3.4±1.8	2.3±0.7	4.2±1.9	.004	<.001	<.001	<.001
Size, cm[a]	7.4±4.1	6.6±3.8	9.4±4.4	.38	4.8±2.7	4.2±1.5	5.2±3.2	.69	.008	.02	.04

NF1 indicates neurofibromatosis type 1; NF, neurofibroma; SWN, schwannoma; SUV_{max}, maximum standardized uptake value.

[a]Mean ± standard deviation (range).

Cancer. Author manuscript; available in PMC 2011 October 7.